HHS Public Access

Author manuscript

Life Sci. Author manuscript; available in PMC 2025 January 01.

Published in final edited form as:

Life Sci. 2024 January 01; 336: 122317. doi:10.1016/j.lfs.2023.122317.

Inhibition of microRNA-34c reduces detrusor ROCK2 expression and urinary bladder inflammation in experimental cystitis

Mousumi Mandal[1], **Ahmed Rakib**[1], **Sonia Kiran**[1], **Md Abdullah Al Mamun**[1], **Somasundaram Raghavan**[1], **Santosh Kumar**[1], **Bhupesh Singla**[1], **Frank Park**[1], **M. Dennis Leo**[*,1], **Udai P. Singh**[*,1]

[1]Department of Pharmaceutical Sciences, College of Pharmacy, 881 Madison Avenue, The University of Tennessee Health Science Center Memphis, TN 38163 USA

Abstract

Interstitial cystitis (IC), also called painful bladder syndrome (PBS), is 2 to 5 times more common in women than in men, yet its cause and pathogenesis remain unclear. In our study using the cyclophosphamide (CYP) induced mouse model of cystitis, histological evaluation of the urinary bladder (UB) lamina propria (LP) showed immune cell infiltrations, indicating moderate to severe inflammation. In this study, we noticed a differential expression of a subset of microRNAs (miRs) in the UB cells (UBs) of CYP-induced cystitis as compared to the control. UB inflammatory scores and inflammatory signaling were also elevated in CYP-induced cystitis as compared to control. We identified eight UBs miRs that exhibited altered expression after CYP induction and are predicted to have a role in inflammation and smooth muscle function (miR-34c-5p, -34b-3p, -212-3p, -449a-5p, -21a-3p, -376b-3p, -376b-5p and -409-5p). Further analysis using ELISA for inflammatory markers and real-time PCR (RT-PCR) for differentially enriched miRs

[*]Corresponding author: Udai P. Singh, Ph.D. and M. Dennis Leo, Ph.D., Department of Pharmaceutical Sciences, College of Pharmacy, 881 Madison Avenue, The University of Tennessee Health Science Center Memphis, TN 38163 USA, usingh1@uthsc.edu and mleo@uthsc.edu.

Author Contributions

Mousumi Mandal, Ahmed Rakib, Sonia Kiran, and Md Abdullah Al Mamun: performed the majority of the experiments, and data analysis, wrote the first draft of the manuscript, and made all the figures; **Somasundaram Raghavan**: performed the western blot helped in data analysis; **Santosh Kumar, Bhupesh Singhla**; edited the mansucript; **Frank Park** has performed the urinary bladder histology; **Udai P Singh** and **Dennis M. Leo**: conceived the idea, design the experiment and edit the manuscript.

The U.S. and DL conceived the idea, designed the experiment, and edited the manuscript. MM, AR, SK, and AM performed the experiment, performed the majority of the experiments, and data analysis wrote the first draft of the manuscript, and made all the figures. SR performed the western blot, and data analysis, and edited the manuscript. FP performed the histological analysis. SK and BS provided the critical editing of the manuscript.

Declaration of Competing Interest

The authors declare that they do not have any competing interests that might influence the outcome of this study or personal relationships that could have appeared to influence the work reported in this paper.

Ethics Statement

All animal experimentation was performed under a protocol number (UPS 23-0450) approved by the University of Tennessee Health Science Center (UTHSC) Institutional Animal Care and Use Committee (IACUC). All animal handling and experimental procedures involving animals were performed to minimize pain and discomfort.

All animal experimentation was performed under a protocol number (UPS 20-0162) approved by the University of Tennessee Health Science Center (UTHSC) Institutional Animal Care and Use Committee (IACUC). All animal handling and experimental procedures involving animals were performed to minimize pain and discomfort.

identified miR-34c as a potential target for the suppression of UB inflammation in cystitis. Blocking miR-34c by antagomir *ex vivo* reduced STAT3, TGF-β1, and VEGF expression in the UBs, which was induced during cystitis as compared to control. Interestingly, miR-34c inhibition also downregulated ROCK2 but elevated ROCK1 expression in bladder and detrusor cells. Thus, the present study shows that targeting miR-34c can mitigate the STAT3, TGF-β, and VEGF, inflammatory signaling in UB, and suppress ROCK2 expression in UBs to effectively suppress the inflammatory response in cystitis. This study highlights miR-34c as a potential biomarker and/or serves as the basis for new therapies for the treatment of cystitis.

Graphics Abstract

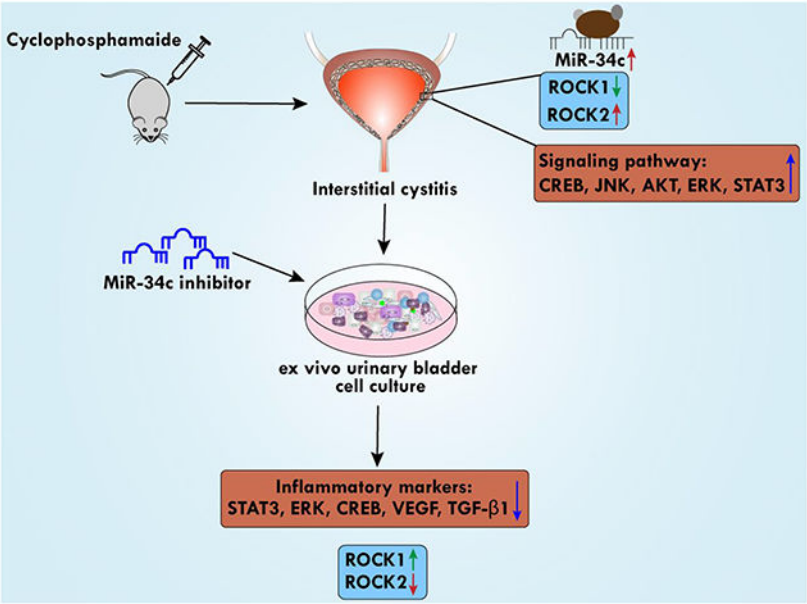

Keywords

Urinary bladder; inflammation; cystitis; microRNAs; ROCK2

Introduction

Interstitial cystitis (IC), also known as painful bladder syndrome (PBS), affects nearly 8 million women and 4 million men in the U.S., yet its cause and pathogenesis remain unclear [1]. IC patients suffer from urinary bladder pain, psychological stress, anxiety, depression, insomnia, and negative work performance. Currently, available treatments reduce IC symptoms but induce lots of side effects including nausea, gastrointestinal distress, and diarrhea. Thus, therapies for the future must depend on pathogenesis and better clarification of the mechanisms that lead to the development of IC. The principal etiology of IC appears to involve an increase in the local adaptive immune response, and the number of T cells, mast cells, and neutrophils in the urinary bladder (UB) [2]. Therefore, we reasoned that at least one stage in the process of developing cystitis must be amenable to immune modulators and other anti-inflammatory therapies. Current animal models have advanced

our understanding of cystitis pathogenesis, but no previous model of bladder injury in healthy experimental animals completely mimicked the salient features of human IC. To this end in this study, we will use a well-established cyclophosphamide (CYP)-induced mouse model of cystitis that represents a significant advance in the field [3]. This model displays many of the clinical characteristics of human IC, including urinary frequency, decreased urine output per void, pelvic nociception, and histopathological alterations such as urothelial cell detachment and increased bladder permeability with epithelial leakage [4]. Thus, a thorough understanding of IC pathogenesis using a CYP-induced model of cystitis will greatly advance our understanding of the mechanisms that underlie cystitis. Further, this will aid in the identification of better diagnostic tools for the development of safe and effective cystitis therapeutic options.

microRNAs (miRs) serve as crucial regulators of both innate and adaptive immune responses and have been linked to many autoimmune diseases, including cystitis. miRs play a key role in various biological processes and differential expression of miRs might be crucial for regulating inflammatory immune effector functions during cystitis. We have shown that expression of specific UB cells (UBs) miRs alters in an autoimmune-induced model of cystitis [5], and dysregulation of miR-155 induces Th1/Th17 polarization and protects mice from intestinal inflammation [6]. It has been shown that dysregulation in miR-34c enhances the development of atherosclerosis [7]. Further, miR-34c suppresses the proliferation of vascular smooth cells via modulating high mobility group box protein 1 and targeting stem cell factors [8, 9]. miR-34c also inhibits differentiation and valvular interstitial cell calcification in calcific aortic valve disease [10]. Thus, this study will determine how miR-34c suppression alters UBs inflammatory and signaling response to reduce the symptoms of IC.

Pathological evaluation of the UB lamina propria shows T cells, macrophage, neutrophils, and mast cell infiltration and granulation, indicating moderate to severe inflammation [11, 12]. The inflammation involves various signaling pathways and inflammatory mediators. Towards this, the cyclic adenosine monophosphate response element binding protein (CREB) is a representative transcription factor and cystitis induces altered CREB expression related to micturition reflex [13]. The c-Jun N-terminal kinase-signal transducer and activator of transcription (JAK-STAT) pathway, are the most studied in various physiological processes including cell growth, differentiation, and immune response. The protein level and constitutive activation of STAT3 have been reported in bladder cancer [14], and STAT3/5 inhibitors suppress bladder cancer [15]. Similarly, the expression and function of transforming growth factor-β (TGF-β) alter in the rat urinary bladder following CYP-induced IC [16]. Several reports show that nitric oxide (NO) plays a significant role in the induction of CYP-induced IC and iNOS is responsible for inflammatory changes in the bladder [17]. The vascular endothelial growth factors (VEGF) are expressed in the urothelial, LP within the bladder wall under normal conditions, but increase during inflammation and pathological conditions [18, 19]. Further, blocking VEGF/VEGER2 signaling suppresses CYP-induced IC in rat UB [20]. To the best of our knowledge, no information is available to date on how miRs expression mediates alteration in CREB, STAT3, iNOS, TGF-β, and VEGF in CYP-induced cystitis.

The major symptoms of cystitis, including frequent urination, urge to urinate, and pain during urination [21], are linked to increased detrusor smooth muscle (DSM) contractions. The DSM contractions mediate various Ca^{2+} channels and any deviation in the omnipresent balance between these channel activities can lead to over-or under-activity of the DSM. IC triggers intense detrusor contractions, but the molecular mechanisms underlying these contractions have remained elusive. Rho-associated protein kinase (ROCK) belongs to the serine/threonine kinases family and plays an important role in cell contraction, motility, proliferation, migration, and leading to cardiovascular disease [22]. The two isoforms, ROCK1 and ROCK2 expressed in circulating inflammatory cells and vascular smooth muscle cells respectively [23, 24] mediate different functions in different types of cells. We noticed that miR-34c increased in UBs in CYP-induced cystitis, but the pathogenesis of cystitis remains unclear. Thus, the main goal of this study is to determine a mechanism that how miR-34c inhibition mediates the bladder inflammatory response during cystitis. The identification of miR-34c involved in the progression of cystitis and targeting miR-34c might represent a novel approach to the prevention and treatment of UB inflammation during cystitis and might be used as a non-invasive biomarker for cystitis-like conditions.

Materials and Methods

Animals and study design

Wild-type C57BL/6 female mice (6-8 weeks old) were purchased from Jackson Laboratories (Bar Harbor, ME, USA) and housed in a specific pathogen-free animal facility at the University of Tennessee Health Science Center (UTHSC), Memphis with normal 12/12 h light/dark cycles. The mice were housed for a week for acclimatization to the animal facility before starting the experiment. All animal experimentation was performed under protocols (20-0169) approved by the University of Tennessee Health Science Centre (UTHSC) Institutional Animal Care and Use Committee (IACUC). Following one week of acclimatization, the mice were randomly divided into two experimental groups and each group contained 5 mice (n = 5) viz., control and cyclophosphamide (CYP) group. Four doses of intraperitoneal (i.p.) injection of cyclophosphamide 80 mg/kg body weight of mouse were given to the CYP group on alternate days (days 2, 4, 6, 8) and i.p. injections of saline were given to the control group. The study was repeated three times. The body weight of mice was measured every day. Mouse behavior (grooming, guarding) was monitored daily. On the last injection day, mice were sacrificed after four hours of injection for collection of the UB for further downstream experiments.

CYP-induced cystitis UB tissue homogenate inflammatory marker analysis by Luminex™

Levels of inflammatory signaling molecules/mediators like JNK, CREB, p38, ERK1/2, STAT-5, STAT-3, NF-kB, AKT, and p70S6k in the UB tissue homogenate were determined using a Luminex plex Elissa assay kit (Millipore, Sigma USA). We previously described the detailed method in our earlier publication [6]. In brief, assay buffer containing beads specific to these targets and 50 µl of assay beads were added into pre-wet vacuum wells, the assay buffer was removed, and the plate was washed with wash buffer. We added 50 µl of the sample (standard, blank, or UB tissue homogenate) to each well and incubated for 1 hour with continuous shaking using a Lab-Line™ Titer Plate Shaker (Melrose, IL). The filter

bottom plates were washed and vortexed at 300x g for 30 seconds. Subsequently, 25 μl of anti-mouse detection antibodies were added to each well and incubated for 30 minutes at room temperature. Next, 50 μl of the streptavidin-phycoerythrin solution was added to each well and incubated with continuous shaking for 10 minutes at RT. Finally, 125 μl of assay buffer was added to each well, and fluorescence was measured using a Luminex™ System (Austin, TX) and calculated using BioRad software.

Urinary bladder single-cell isolation

At the experimental endpoint, single-cell suspensions were prepared from the urinary bladder (UB) obtained from each group of mice. UB cells were dissociated by stomacher in RPMI 1640 (Corning 10-041-CV, USA) with 10% FBS. After centrifugation, cell suspensions of UB were passed through a sterile 70μM filter (Genesee, USA) to prepare a single-cell suspension. Cell counts were taken in Countess 3 automated cell counter (ThermoFisher Scientific, USA) by using trypan blue and used for the downstream experiment. The cells were kept at 4°C for further analysis.

miRNAs isolation and microarray analysis

Initially, UB tissues were dissociated with a tissue homogenizer and miRs with total RNA were isolated by a miRNeasy mini kit (QIAGEN, Valencia, CA). miRs were isolated according to the manufacturer's instructions and samples were stored at −80°C before being sent to the Johns Hopkins University sequencing core facility for microarray analysis. Total RNA from UB including miRNAs was hybridized to an Affymetrix Gene Chip high throughput miR array containing 609 murine probes (Affymetrix, Santa Clara, CA). The data generated from the array were analyzed using hierarchical clustering. By use of ingenuity pathway analysis (IPA) software (Qiagen; www.ingenuity.com), the results from the miRs microarray were analyzed to identify molecular pathways potentially altered by single or multiple miRs target genes. In brief, this analysis compares each set of miRs to all available pathways in the database and assigns priority scores based on the predicted strength of the miRs interaction with components of the target pathway.

ex vivo culture and miR-34c-3p inhibitor treatment

We used miR-34c-3p, miR-34c-5p, and miR-34b-3p inhibitors in the UBs and noticed that miR-34c-3p most effectively reduces the inflammatory response, thus used in the entire study. After aseptic isolation of UB single cells were transfected with the combination of miR-34c-inhibitor (Invitrogen, USA Ambion Cat. 4464085, ID MH11039) and Lipofectamine RNAiMAX (Invitrogen, Ref: 13778-030) with manufacturer instruction and culture for 24 hours. In brief, cells were seeded in complete RPMI-1640 media and transfected with 10 nM has-miR34c-3p inhibitor in the final concentration. After 24 hr cells were harvested and proceeded for downstream experiments such as RNA extraction, real-time PCR (RT-PCR), protein isolation, and western blot analysis.

RNA extraction and real-time PCR (RT-PCR)

Total RNA from bladder cells and miR-34c-3p inhibitor transfected bladder cells was extracted by using the RNeasy mini kit (Cat. 74104; QIAGEN, USA). Five hundred

nanograms of extracted RNA in each sample were used for reverse-transcribed cDNA using an iScript cDNA synthesis kit (Cat. 1708891; Bio-Rad, USA) following the manufacturer's protocol. RT-PCR was performed using the iTaq Universal SYBR Green Supermix (Cat. 1725121; Bio-Rad, USA). Primers were purchased from Integrated DNA Technologies (IDT) and QIAGEN. miRCURY LNA RT Kit (339340, QIAGEN, USA) was used for the cDNA preparation of miR. RT-PCR of miRs was performed by miRCURY LNA SYBR Green PCR Kit (339346, QIAGEN). The primer sequence is provided in Tables 1 and 2.

Histopathological examination

Mouse UBs were subjected to histopathological examination to detect inflammatory cell infiltrates and signs of cystitis pathology. UBs were preserved using 10% neutral formalin for 24 hours and embedded in paraffin. Fixed tissues were sectioned at 6 μm, stained with hematoxylin and eosin, and examined by light microscopy. The inflammatory state of each UB was characterized and scored as follows: having no change when compared with tissue samples from control mice (score = 0); having a few mononuclear cell infiltrates (score = 1); having minimal hyperplasia with a mixture of mononuclear cells (score = 2); having major hyperplasia (score = 3) or having major hyperplasia with heavy cellular infiltrates in the sub-mucosa (score = 4).

Protein extraction and Western blot

UB cells were washed twice with cold phosphate-buffered saline (PBS) and lysed with RIPA buffer supplemented with a protease and phosphatase inhibitor cocktail. Cells were ruptured by pipetting, sonicated for 1 min, and incubated on ice for 30 min to ensure complete lysis. For detrusor lysate, the whole bladder was isolated from mice and the urothelium was dissected under a microscope in cold PBS. The detrusor tissue was then homogenized in RIPA buffer. In both cases, after homogenization, cell debris was removed by centrifugation at 15,000 x g for 20 min. The protein concentration of the resulting supernatant was measured with a Pierce™ BCA Protein Assay Kit (ThermoFisher Scientific, Waltham, MA). Equal amounts (50 μg) of protein for each sample were separated by 10% SDS (Sodium Dodecyl Sulfate)-PAGE (polyacrylamide gel electrophoresis) and transferred to nitrocellulose membranes (1620112, Bio-Rad) using Transblot Turbo (Bio-Rad). The membrane was blocked with 5% fat-free milk dissolved in Tris-buffered saline with Tween-20 (TBST) at RT for 1 h and incubated at 4°C overnight on a shaker with primary antibodies specific for ROCK-1 (1:500; cat. no. 4035; Cell Signaling Tech), ROCK-2 (1:500; cat. no. 47012; Cell Signaling Tech), and β-actin (1:5,000; cat. no. MAB1501, EMD Millipore). Unbound primary antibodies were removed by washing with TBST and the membranes were incubated at RT for 1 h with anti-rabbit (1:5000; cat. no. 31470, ThermoFisher) or anti-mouse (1:5,000; cat. no. 7076; Cell Signaling) secondary antibodies. Images were taken Biorad Chemidoc imaging system and densitometric analyses were performed using Image Lab Software.

Statistical analysis

The data are expressed as the mean ± SEM of at least three replicates and were compared using student's *t*-test or one-way ANOVA where traditional α-value ($p < 0.05$) was statistically significant in this study. Graphical representations were generated using

GraphPad Prism (GraphPad Software, Boston, MA) and Origin8 (OriginLab, Northampton, MA) software.

Results

Body weight, wet bladder weight, and UB inflammatory response during CYP-induced cystitis

We examined the changes in body weight, wet bladder weight, and UB inflammation in control and CYP-induced cystitis in mice. CYP induction reduced body weight as compared to saline-treated control mice (Fig. 1A). Further, the wet bladder weight increased in CYP induction relative to control mice (Fig. 1B). The inflammation and inflammatory score determined from UB histology also increased in CYP mice as compared to control mice (Figs. 1C and 1D). Histological examination showed that control mice exhibited normal organized tissue architecture with only very few inflammatory infiltrates in the UB (Fig. 1C; **arrow**). In contrast, the UB histology of mice treated with CYP exhibited chronic inflammation with extensive small to multifocal inflammatory cell infiltrates (Fig. 1C arrow), edema as well and urothelial hyperplasia as compared to control (Fig. 1C). The results suggest that CYP induction might impeded epithelial barrier function that alters UB mucosal immunity and participates in modulating the inflammatory immune response to enhance IC symptoms in the UB.

CYP induction alters the mediators of inflammatory signaling

It has been previously observed that during cystitis, T cells, macrophage, neutrophils, and mast cell infiltration and granulation occur in the UB leading to moderate to severe inflammation [11, 12]. The inflammatory signaling in the UB involves various signaling pathways like CREB, JNK, p38, protein kinase B (AKT), extracellular signal-regulated kinase (ERK), p70S6K, STAT5, and STAT3 pathways. By using a multiplex ELISA assay, we measured that CREB, JNK, p38, AKT, ERK1/2, p70S6K, STAT-5, and STAT-3 signaling was upregulated in the CYP-induced UBs as compared to control (Fig. 2). The data suggest that CYP induced multiple inflammatory signaling in the UB, and suppression of these pathways might be an effective approach to suppress urinary bladder inflammatory response in cystitis.

microRNA (miRs) differential expression in UBs during CYP-induced cystitis

The function of various genes can be altered by epigenetic regulation mediated by miRs. To further define the mechanisms of gene regulation during the progression of CYP-induced cystitis, we isolated total RNA from UBs and performed miRNA arrays in the core facility at the Johns Hopkins School of Medicine, MD. Following global normalization of the raw data, we identified several miRs that were differentially expressed in CYP-treated mice relative to control mice which are depicted in the heatmap (Fig. 3A). We observed distinct patterns of several UBs miRs including miR-34c-5p, miR-21a-3p, miR-34b-3p miR-212-3p, miR-449a-5p, miR-376b-3p, miR-376b-5p, and miR-409-5p, expression in CYP-induced as compared to control, suggesting that cystitis may result from altered miRs expression mediated by CYP induction. Furthermore, the miRs analyzed by the heatmap were then mapped as a dendrogram to show their interaction with different genes like

ankyrin repeat domain 17 (Ankrd17), hypoxia-inducible factor 1 subunit alpha (HIF1α) and PEST Proteolytic Signal Containing Nuclear Protein (PCNP) (Fig. 3B). Additionally, these miRs are involved with various cellular pathways and cancer which was generated by KEGG pathway analysis (Fig. 3C). Since these differentially regulated miRs are involved in colorectal and bladder cancer and high incidence that these miRs might be a bonafide target for therapeutic intervention.

miRNA expression networks and their target validation of miR-34c

We observed upregulation of a set of miRs that includes miRs-34a/b/c, miR-21a, and miR-132-3p. These miRs alter cell proliferation, migration, and several inflammatory signaling pathways. Gene ontology mapping (Fig. 4A) revealed that miR-34c was involved in several critical cellular pathways associated with proliferation and cytoskeletal rearrangement. The expression profiles of all miRs were analyzed by a volcano plot (Fig. 4B) and identified that miR-34c shows the largest fold difference between control and CYP-treated bladder. For this, we first verified that miR-34c-5p and miR-34b-3p expression showed significant increases in CYP induction as compared to control (Fig. 4C). Our results suggest that cystitis induction and progression might be related to CYP-induced differential expression of miR-34c which modulates the function of various inflammatory pathways. Taken together, these microarray and RT-qPCR data strongly suggest a key role for miR-34c in the progression of IC and provide a rationale to determine whether alteration of these miRs enhances/suppresses the symptoms of IC. Based on this and the potency of *in vitro* inhibition of inflammatory response, we selected miR-34c-3p for further *ex vivo* manipulation since their associated gene network targets are crucial for cystitis progression.

Validation of dysregulated miRs expression in CYP-induced UBs

Next, we verified several dysregulated miRs expressions in CYP UB tissue after CYP induction. RNA was isolated from UBs and real-time PCR was performed for the top dysregulated miRs that we identified previously. Based on the inflammatory pathways and prediction, we validated key results from the microarray analysis, six miRs (miR-212-3p, miR-449a-5p, miR-21a-3p, miR-376b-3p, miR-376b-5p, and miR-409-5p). Among them, miR-212-3p, miR-449a-5p, and miR-21a-3p are upregulated and miR-376b-3p, miR-376b-5p, and miR-409-5p are downregulated in CYP induced IC group compared to control (Fig. 5). Results indicate that the top differentially enriched miRs (miR-212, miR-449a, and miR-21a) of UBs also showed a similar pattern of expression with miR-34c. We selected miR-34c-3p based on the highly predicted based on immune, muscle, and neuropathic pain-mediated signaling pathways.

Targeting miR-34c-3p suppresses inflammatory markers

It has been shown previously that targeting miR-34c was a novel therapeutic strategy for intervention for cardiovascular disease [25]. Further, miR-34 has also been shown to play a crucial role in repressing tumor progression by involving in epithelial-mesenchymal transition (EMT) via EMT-transcription factors, p53, and some important signaling pathways like Notch and TGF-β signaling [26]. Hence, we first tested miR-34c inhibition in UB cells isolated from CYP-treated bladders. miR-34c antagomir was added to the culture media at 10 nM final concentration and allowed to incubate for 24h in a CO_2 incubator

after which RT-PCR was performed for different inflammatory markers mentioned earlier. Interestingly, we noticed a prominent reduction in STAT-3 (Fig. 6) suggesting that STAT3 is a possible downstream target of miR-34c in UB. Furthermore, miR-34c also suppresses other inflammatory genes like ERK and CREB. Although other inflammatory markers like STAT5, Akt, JNK, iNOS, and IL-1β are not significantly altered after miR-34c inhibition, it is likely due to the shorter incubation time of antagomir (24h). The potential for further inhibition of these inflammatory markers needs to be assessed using extended-time course experiments.

Alteration in TGF-β1, VEGF, NGF and PIEZO1 expression after miR-34c-3p inhibition

Next, we also looked at key inflammatory targets involved in proliferation, neuronal signaling, and smooth muscle function. It has been shown that an increase in peripheral TGF-β1 reactivity in chronic inflammatory bladder conditions, and its role in urinary bladder dysfunction influence bladder afferent excitability to amplify nociceptive transmission and CNS input. We examined the effect of miR-34c inhibition during CYP-induced cystitis. Results indicate that miR-34c-3p inhibition reduced TGF-β1 and VEGF levels while NGF and PIEZO1 levels showed no change (Fig. 7). VEGF functions as a potent inflammatory mediator and has been considered an important target for IC [20].

Differential ROCK isoform expression in the detrusor is a possible mediator of increased detrusor contractility.

Next, we wanted to further test the effect of miR-34c modulation on ROCK isoforms. ROCK is essential for smooth muscle contraction. ROCK isoforms play an important role in cell contraction, motility, proliferation, and migration [22]. The two isoforms ROCK1 and ROCK2 are expressed in circulating inflammatory cells and vascular smooth muscle cells respectively [23, 24]. It mediates different functions in different types of cells during inflammation. Since a major IC symptom is pain and the urge to urinate, we postulated that this might be associated with increased expression of one or more ROCK isoforms in the bladder. Accordingly, we used a western blot to determine the change in protein expression. In whole detrusor tissue, CYP induced a decrease in ROCK1 but an increase in ROCK2 (Fig. 8A, B). Similarly, in isolated UB cells, ROCK1 decreased whereas ROCK2 increased after CYP. Isolated cells from the control and CYP-treated bladder were then incubated for 24 h with the miR-34c-3p antagomir. Results indicate no effect in control cells but in CYP cells, miR-34c antagonism restored both ROCK1 and ROCK2 expression (Fig. 8C–E). These results suggest that miR-34c-3p could also alleviate bladder contractile pathways during cystitis. Further, antagonizing miR-34c-3p in the cystitis bladder could potentially suppress inflammatory and detrusor contractility pathways and neuronal overactivity that possibly alleviate the primary symptoms of cystitis.

Discussion

The etiology and pathogenesis of interstitial cystitis are not fully known, but studies linking several autoimmune etiologies with cystitis and inflammation including epithelial dysfunction, neurogenic upregulation, infection, and bladder inflammation have emerged as key constitutive elements in the events cascade of cystitis [27]. In this study, we identified a

set of altered miRs during CYP-induced cystitis and uncovered that miR-34c is significantly increased in the UBs of IC mice as compared to the control. Hence, the goal of this study was to determine if inhibition of miR-34c-3p suppresses the inflammatory response of IC. In this study, we demonstrated that inhibition of miR-34c-3p reduced the STAT3, TGF-β1, VEGF, and ROCK2 expression in UB cells, which effectively suppresses IC. This study will provide miR-34c-3p as potential biomarkers and/or serve as the basis for new therapies for the treatment of IC.

It has been established that miRs can regulate multiple genes by binding to target mRNAs, thereby controlling the stability and translation of protein-coding mRNAs [28, 29]. miRs expressed in many peripheral tissues including the colon and can regulate inflammation [30, 31]. We have shown that differential expression of miRs correlates with the severity of experimental autoimmune cystitis [5]. In this study, we noticed several miRs also dysregulated in the UBs isolated from the CYP-induced mice compared to the control. Several putative targets of these miRs are related to the inflammatory, neuropathic pain, and detrusor smooth muscle function process. Among them, based on the pathway prediction we, selected miR-34c for further analysis during IC. miR-34c is associated with diverse functions like enhancing wound inflammation by regulating keratinocyte inflammatory response targeting Leucine-rich repeat-containing G-protein coupled receptor 4 [32] and inhibiting smooth muscle cell function [8].

In this study, we uncovered that miR-34c antagomir treatment remarkably reduces the expression of STAT3, ERK, CREB, TGF-β1, and VEGF as compared to the scramble miRs. STAT3 has been shown as one of the potent transcription factors for inflammatory pathways activated by various pro-inflammatory cytokines [33]. Further, ERK is known to be involved with chronic inflammation [34]. CREB is involved in Th17 cell differentiation and regulatory T (Treg) cell inhibition [35]. TGF-β1 is a pleiotropic cytokine that has both pro and anti-inflammatory functions depending on the context of the disease [36]. However, higher expression of VEGF was shown to be associated with cystitis, and targeting VEGF signaling might be an effective treatment for IC [20]. ROCK kinase isoform functions in both inflammatory cells and smooth muscle. In recent studies, serum levels of ROCK2 were found to increase in patients with overactive bladder [37] and although both isoforms are known to be present in the bladder, it is speculated that ROCK2 is likely involved with increased detrusor contraction in cystitis and other bladder diseases [38]. Our data here also shows that ROCK1 is the likely constitutive form of the kinase whereas ROCK2 appeared to be upregulated during IC when miR-34c antagonism reverted. Taken together, our data corroborate previous studies [37] and suggest that the miR-34c inhibition effectively reduces bladder inflammation and contractility through STAT3, CREB, TGF-β1, VEGF, and ROCK2 pathways and likely alleviates the primary symptoms of IC to restore normal UB function.

miR-34 family has been known for tumor suppressive function, including proliferation, migration, and invasion while promoting senescence and apoptosis [39]. In recent years several studies have suggested the therapeutic effect of miR-34c in suppressing atherosclerosis by decreasing the expression of high mobility group box protein 1 [8]. miR-34 family also attenuates pathological cardiac remodeling and improves heart function [40]. Further, overexpressing miR-34c inhibits radio-resistant nasopharyngeal carcinoma and

protects against cerebral ischemia-reperfusion injury through anti-inflammatory cytokines activities [41]. Our data suggest that miR-34c inhibition reduces the inflammatory markers (STAT3, ERK, and TGF-β1) in the UB to suppress inflammation of IC. These data pave the way for further in-depth studies on the possibility of miR-34c therapeutics for IC and other inflammatory models.

Supplementary Material

Refer to Web version on PubMed Central for supplementary material.

Acknowledgment

This study was supported by grants from NIH (NIAID R01 AI140405) to the U.S. at UTHSC in Memphis, TN.

Funding and Disclosure:

All authors have nothing to disclose.

Data Availability Statement

The raw and processed data reported in this paper are available in the Gene Expression Omnibus (GEO) repository with accession number GSE243239. The data supporting the conclusions including the miRNAs expression and analysis data of this manuscript will be made available to the public by the authors, without any reservation.

This paper's raw and processed data are available in the Gene Expression Omnibus (GEO) repository with accession number GSE243239. The authors will make the data supporting the microRNA conclusions, and flow cytometry data, including this manuscript's, will be available to the public, without any reservation.

References

1. Nordling J, Fall M, Hanno P: Global concepts of bladder pain syndrome (interstitial cystitis). World J Urol 2012, 30(4):457–464. [PubMed: 22057291]
2. Gamper M, Viereck V, Eberhard J, Binder J, Moll C, Welter J, Moser R: Local immune response in bladder pain syndrome/interstitial cystitis ESSIC type 3C. Int Urogynecol J 2013, 24(12):2049–2057. [PubMed: 23670165]
3. Lin YH, Liu G, Kavran M, Altuntas CZ, Gasbarro G, Tuohy VK, Daneshgari F: Lower urinary tract phenotype of experimental autoimmune cystitis in mouse: a potential animal model for interstitial cystitis. BJU international 2008, 102(11):1724–1730. [PubMed: 18710451]
4. Singh UP, Singh NP, Guan H, Hegde VL, Price RL, Taub DD, Mishra MK, Nagarkatti M, Nagarkatti PS: The severity of experimental autoimmune cystitis can be ameliorated by anti-CXCL10 Ab treatment. PLoS One 2013, 8(11):e79751. [PubMed: 24278169]
5. Kumar V, Kiran S, Shamran HA, Singh UP: Differential Expression of microRNAs Correlates With the Severity of Experimental Autoimmune Cystitis. Front Immunol 2021,12:716564. [PubMed: 34335632]
6. Singh UP, Murphy AE, Enos RT, Shamran HA, Singh NP, Guan H, Hegde VL, Fan D, Price RL, Taub DD: miR-155 deficiency protects mice from experimental colitis by reducing T helper type 1/type 17 responses. Immunology 2014, 143(3):478–489. [PubMed: 24891206]
7. Murakami Y, Yasuda T, Saigo K, Urashima T, Toyoda H, Okanoue T, Shimotohno K: Comprehensive analysis of microRNA expression patterns in hepatocellular carcinoma and non-tumorous tissues. Oncogene 2006, 25(17):2537–2545. [PubMed: 16331254]

8. Chen LB, An Z, Zheng HK, Wang XP, Shan RT, Mao CY, Zhang WQ: MicroRNA-34c suppresses proliferation of vascular smooth muscle cell via modulating high mobility group box protein 1. J Clin Lab Anal 2020, 34(7):e23293. [PubMed: 32157741]
9. Choe N, Kwon JS, Kim YS, Eom GH, Ahn YK, Baik YH, Park HY, Kook H: The microRNA miR-34c inhibits vascular smooth muscle cell proliferation and neointimal hyperplasia by targeting stem cell factor. Cellular signalling 2015, 27(6):1056–1065. [PubMed: 25683915]
10. Yang L, Zhu X, Ni Y, Wu D, Tian Y, Chen Z, Li M, Zhang H, Liang D: MicroRNA-34c Inhibits Osteogenic Differentiation and Valvular Interstitial Cell Calcification via STC1-Mediated JNK Pathway in Calcific Aortic Valve Disease. Front Physiol 2020, 11:829. [PubMed: 32982764]
11. Vysakh A, Suma D, Jayesh K, Jyothis M, Latha MS: The influence of tissue antioxidant enzymes and inflammatory cascade in pathology of cystitis: An experimental rat model. Microb Pathog 2017, 113:102–106. [PubMed: 29066378]
12. Lin HC, Lee HS, Chiueh TS, Lin YC, Lin HA, Lin YC, Cha TL, Meng E: Histopathological assessment of inflammation and expression of inflammatory markers in patients with ketamine-induced cystitis. Mol Med Rep 2015, 11(4):2421–2428. [PubMed: 25523514]
13. Choi T, Lee DG: Cystitis Induces Altered CREB Expression Related with Micturition Reflex. Medicina (Kaunas) 2022, 58(9).
14. Gatta LB, Melocchi L, Bugatti M, Missale F, Lonardi S, Zanetti B, Cristinelli L, Belotti S, Simeone C, Ronca R et al. Hyper-Activation of STAT3 Sustains Progression of Non-Papillary Basal-Type Bladder Cancer via FOSL1 Regulome. Cancers (Basel) 2019, 11(9).
15. Hindupur SV, Schmid SC, Koch JA, Youssef A, Baur EM, Wang D, Horn T, Slotta-Huspenina J, Gschwend JE, Holm PS et al. STAT3/5 Inhibitors Suppress Proliferation in Bladder Cancer and Enhance Oncolytic Adenovirus Therapy. Int J Mol Sci 2020, 21(3).
16. Gonzalez EJ, Girard BM, Vizzard MA: Expression and function of transforming growth factor-beta isoforms and cognate receptors in the rat urinary bladder following cyclophosphamide-induced cystitis. Am J Physiol Renal Physiol 2013, 305(9):F1265–1276. [PubMed: 23926183]
17. Alfieri AB, Malave A, Cubeddu LX: Nitric oxide synthases and cyclophosphamide-induced cystitis in rats. Naunyn Schmiedebergs Arch Pharmacol 2001, 363(3):353–357. [PubMed: 11284451]
18. Kiuchi H, Tsujimura A, Takao T, Yamamoto K, Nakayama J, Miyagawa Y, Nonomura N, Takeyama M, Okuyama A: Increased vascular endothelial growth factor expression in patients with bladder pain syndrome/interstitial cystitis: its association with pain severity and glomerulations. BJU international 2009, 104(6):826–831; discussion 831. [PubMed: 19298410]
19. Malykhina AP, Lei Q, Erickson CS, Epstein ML, Saban MR, Davis CA, Saban R: VEGF induces sensory and motor peripheral plasticity, alters bladder function, and promotes visceral sensitivity. BMC Physiol 2012, 12:15. [PubMed: 23249422]
20. Tooke K, Girard B, Vizzard MA: Functional effects of blocking VEGF/VEGFR2 signaling in the rat urinary bladder in acute and chronic CYP-induced cystitis. Am J Physiol Renal Physiol 2019, 317(7):F43–F51. [PubMed: 30995112]
21. Rudick CN, Schaeffer AJ, Klumpp DJ: Pharmacologic attenuation of pelvic pain in a murine model of interstitial cystitis. BMC Urol 2009, 9:16. [PubMed: 19909543]
22. Shimokawa H, Rashid M: Development of Rho-kinase inhibitors for cardiovascular medicine. Trends Pharmacol Sci 2007, 28(6):296–302. [PubMed: 17482681]
23. Chevrier V, Piel M, Collomb N, Saoudi Y, Frank R, Paintrand M, Narumiya S, Bornens M, Job D: The Rho-associated protein kinase p160ROCK is required for centrosome positioning. J Cell Biol 2002, 157(5):807–817. [PubMed: 12034773]
24. Wei L, Roberts W, Wang L, Yamada M, Zhang S, Zhao Z, Rivkees SA, Schwartz RJ, Imanaka-Yoshida K: Rho kinases play an obligatory role in vertebrate embryonic organogenesis. Development 2001, 128(15):2953–2962. [PubMed: 11532918]
25. Hua CC, Liu XM, Liang LR, Wang LF, Zhong JC: Targeting the microRNA-34a as a Novel Therapeutic Strategy for Cardiovascular Diseases. Front Cardiovasc Med 2021, 8:784044. [PubMed: 35155600]
26. Zhang L, Liao Y, Tang L: MicroRNA-34 family: a potential tumor suppressor and therapeutic candidate in cancer. Journal of experimental & clinical cancer research : CR 2019, 38(1):53. [PubMed: 30717802]

27. Sant GR: Etiology, pathogenesis, and diagnosis of interstitial cystitis. Rev Urol 2002, 4 Suppl 1(Suppl 1):S9–S15.
28. Guo H, Ingolia NT, Weissman JS, Bartel DP: Mammalian microRNAs predominantly act to decrease target mRNA levels. Nature 2010, 466(7308):835–840. [PubMed: 20703300]
29. Esteller M: Non-coding RNAs in human disease. Nature reviews Genetics 2011, 12(12):861–874.
30. Ambros V: The functions of animal microRNAs. Nature 2004, 431(7006):350–355. [PubMed: 15372042]
31. O'Connell RM, Rao DS, Baltimore D: microRNA regulation of inflammatory responses. Annu Rev Immunol 2012, 30:295–312. [PubMed: 22224773]
32. Wu J, Li X, Li D, Ren X, Li Y, Herter EK, Qian M, Toma MA, Wintler AM, Serezal IG et al. MicroRNA-34 Family Enhances Wound Inflammation by Targeting LGR4. J Invest Dermatol 2020, 140(2):465–476 e411. [PubMed: 31376385]
33. Hillmer EJ, Zhang H, Li HS, Watowich SS: STAT3 signaling in immunity. Cytokine Growth Factor Rev 2016, 31:1–15. [PubMed: 27185365]
34. Lu N, Malemud CJ: Extracellular Signal-Regulated Kinase: A Regulator of Cell Growth, Inflammation, Chondrocyte and Bone Cell Receptor-Mediated Gene Expression. Int J Mol Sci 2019, 20(15).
35. Wang X, Ni L, Chang D, Lu H, Jiang Y, Kim BS, Wang A, Liu X, Zhong B, Yang X et al. Cyclic AMP-Responsive Element-Binding Protein (CREB) is Critical in Autoimmunity by Promoting Th17 but Inhibiting Treg Cell Differentiation. EBioMedicine 2017, 25:165–174. [PubMed: 29050947]
36. Han G, Li F, Singh TP, Wolf P, Wang XJ: The pro-inflammatory role of TGFbeta1: a paradox? Int J Biol Sci 2012, 8(2):228–235. [PubMed: 22253566]
37. Firat E, Aybek Z, Aybek H: ADRB3, ROCK2, and GEF Levels in Overactive Bladder Patients. Int Neurourol J 2022, 26(Suppl 1):S8–14. [PubMed: 35236048]
38. Matoba K, Takeda Y, Nagai Y, Sekiguchi K, Yokota T, Utsunomiya K, Nishimura R: The Physiology, Pathology, and Therapeutic Interventions for ROCK Isoforms in Diabetic Kidney Disease. Front Pharmacol 2020, 11:585633. [PubMed: 33101039]
39. Misso G, Di Martino MT, De Rosa G, Farooqi AA, Lombardi A, Campani V, Zarone MR, Gulla A, Tagliaferri P, Tassone P et al. Mir-34: a new weapon against cancer? Mol Ther Nucleic Acids 2014, 3(9):e194.
40. Bernardo BC, Gao XM, Winbanks CE, Boey EJ, Tham YK, Kiriazis H, Gregorevic P, Obad S, Kauppinen S, Du XJ et al. Therapeutic inhibition of the miR-34 family attenuates pathological cardiac remodeling and improves heart function. Proc Natl Acad Sci U S A 2012, 109(43):17615–17620. [PubMed: 23047694]
41. Tu Y, Hu Y: MiRNA-34c-5p protects against cerebral ischemia/reperfusion injury: involvement of anti-apoptotic and anti-inflammatory activities. Metab Brain Dis 2021, 36(6):1341–1351. [PubMed: 33842985]

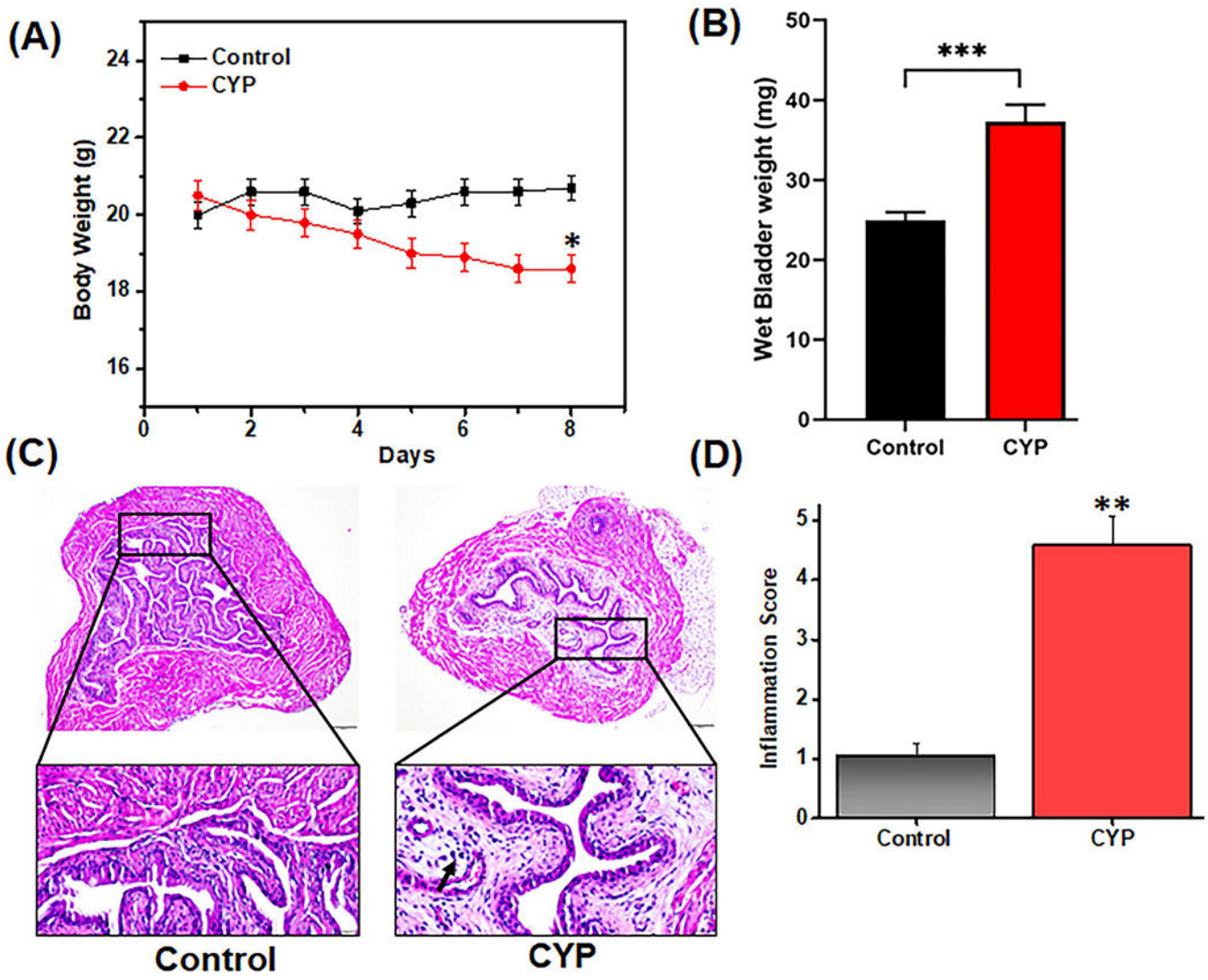

Fig. 1. Cyclophosphamide (CYP) induced cystitis alters body weight, urinary bladder weight, histological, and inflammation score

C57BL/6 control mice (■) received normal saline, (●) received CYP (80 mg/kg body weight) on alternate days (days 2, 4, 6, 8) by i.p. injections. The body weight of the mice was recorded every day. (A) shows a representative plot of body weight changes after CYP induction. Body weight declined in the CYP group compared to control. (B) Mice were sacrificed after eight days and the wet bladder weight was recorded. The increment of UB weight in the CYP group was noticed as compared to the control. (C) Histological microphotographs of UB from CYP-induced and control mice are shown. Mice that received CYP showed cellular infiltration and reduced lumen space as compared to control mice. (D) The mean UB inflammation score from CYP-induced cystitis and control is shown in the plot. All data represent the mean ± SEM from three independent experiments involving 5 mice per group (n=5). Asterisks indicate statistically significant differences between control and CYP-induced cystitis (⋆$p<0.05$, ⋆⋆$p<0.01$, and ⋆⋆⋆$p<0.001$).

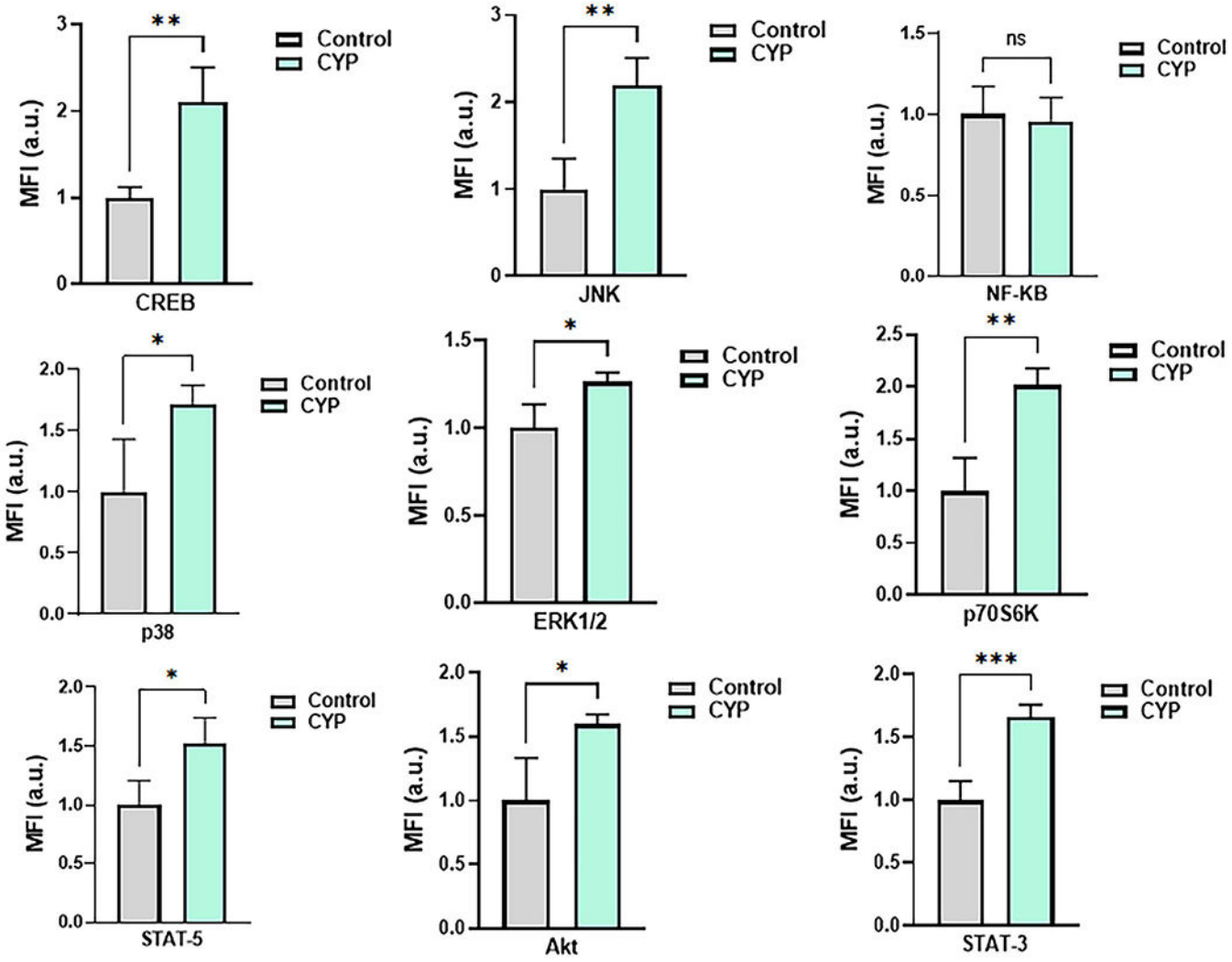

Figure 2. CYP induces inflammatory and mitogen-activated kinase pathways in UB

The urinary bladder from two groups of mice was collected at the experimental endpoint and tissue homogenate was prepared by centrifugation in lysis buffer (Millipore Sigma, USA). Inflammatory signalings pathways CREB, JNK, NF-kB, p38, ERK1/2, p70S6K, STAT5, AKT, and STAT3 in the UB tissue homogenate were determined using a Luminex plex ELISA assay kit (Millipore, Sigma USA). Data represent the MFI (a.u) of inflammatory pathways ± SEM from the three independent experiments. Except for NF-kB, all other signaling molecules are significantly elevated in the CYP-induced cystitis as compared to the control group. Asterisks indicate statistically significant differences between control and CYP-induced groups (ns= not significant $p > 0.05$, ⋆$p < 0.05$, ⋆⋆$p<0.01$ and ⋆⋆⋆$p<0.001$).

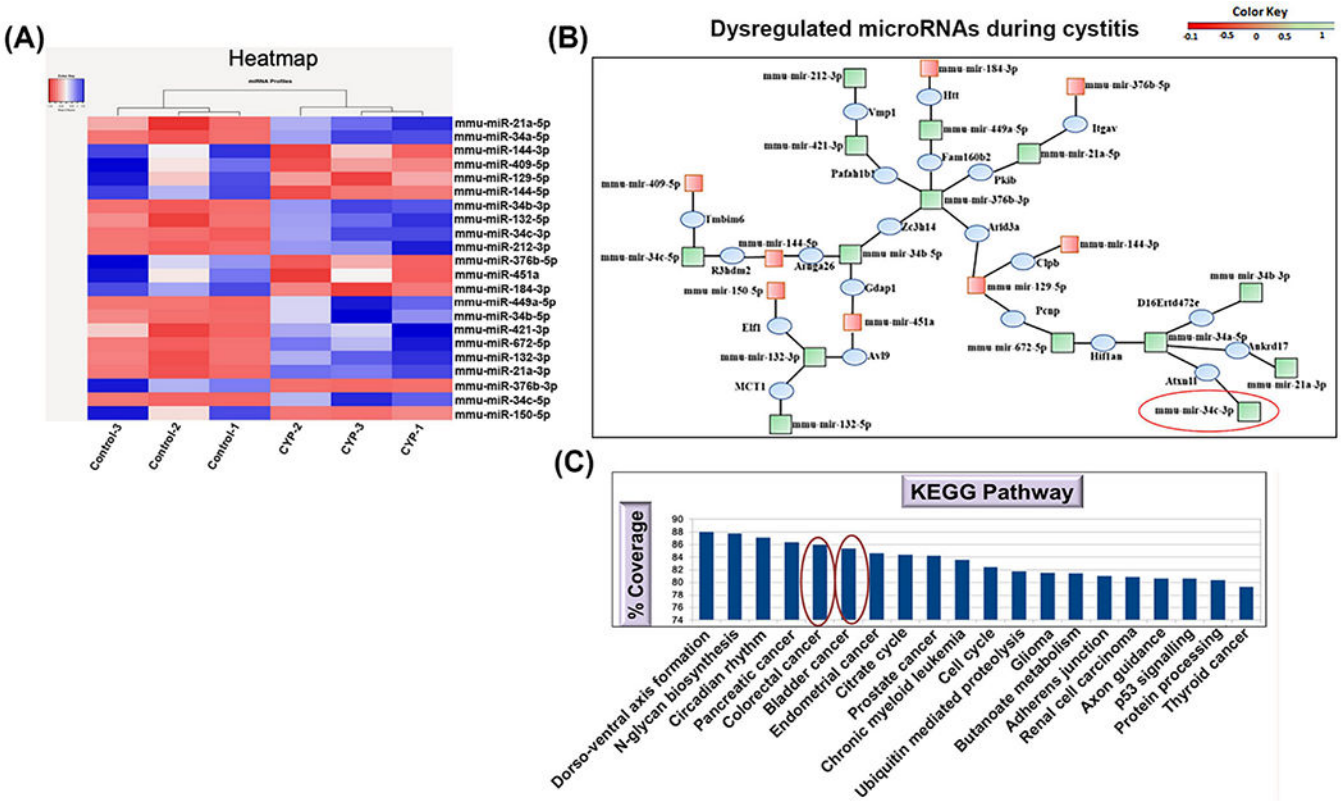

Figure 3. CYP alters the UBs cell's miRs expressions

Effect of CYP induction on miRs expression in urinary bladder cells. Changes in unsupervised hierarchical clustering of differentially expressed miRs in CYP-induced cystitis versus control mice-derived UB cells reveal divergent pathways. (A) Heat map showing altered expression of the miRs in UB cells from CYP-induced versus control mice. Five biological samples were pooled for the miRs analysis, but all validation was performed in individual samples. (B) Dendrogram generated from ingenuity pathways analysis (IPA) in the top most dysregulated miRs in UB during CYP-induced cystitis. The red color indicates an upregulation and the green color indicates a downregulation of miRs expression. (C) KEGG pathway analysis using Ingenuity software during CYP-induced cystitis miRs associated with bladder and colorectal cancer.

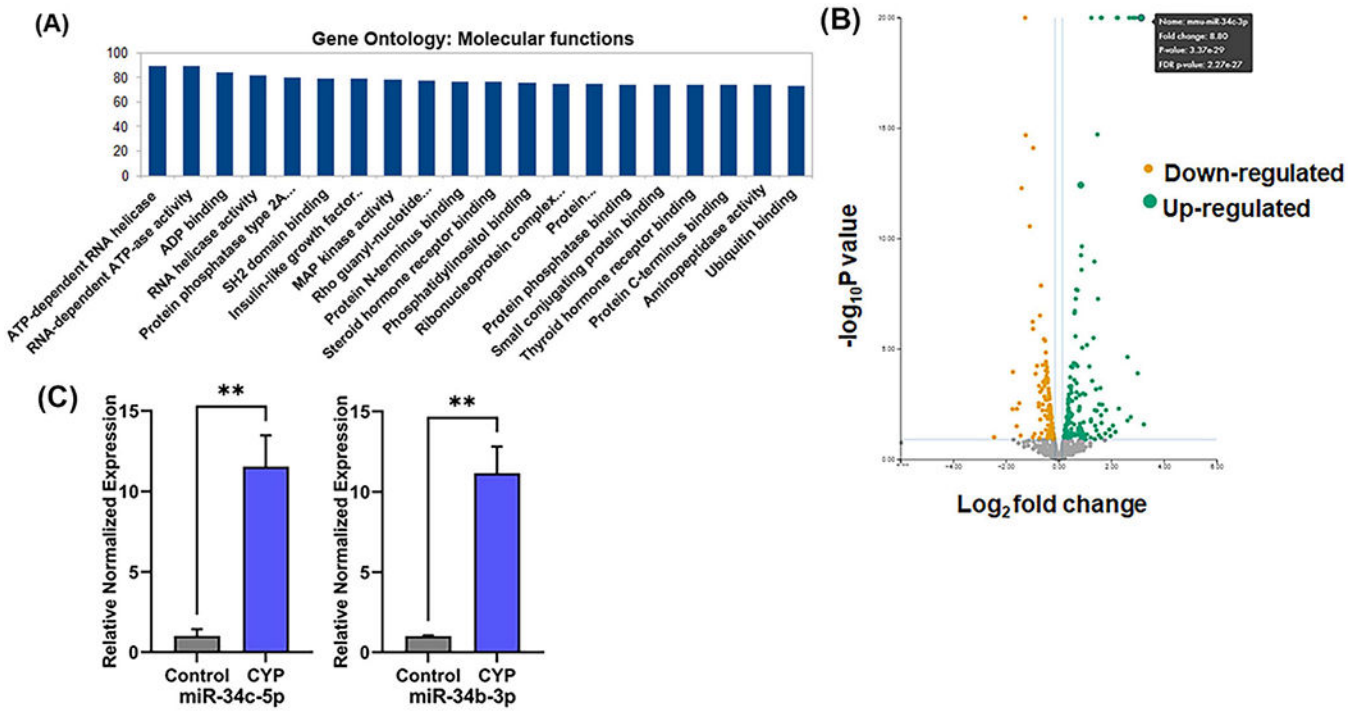

Figure 4. Selection and validation of miR-34c after CYP-induced cystitis

(A) Top ingenuity pathways analysis (IPA) overlapping gene ontology and molecular function. (B) The volcano plot shows overexpression of miR-34c-3p after CYP-induced cystitis. (C) Quantitative RT-PCR verifying upregulation of miR-34c-5p and miR-34b-3p in UB after CYP-induced cystitis. Data are expressed as mean ± SEM. Statistical significance was calculated using the Student's t-test between control and CYP-induced cystitis groups. (⋆ ⋆$p < 0.01$) control vs. cystitis.

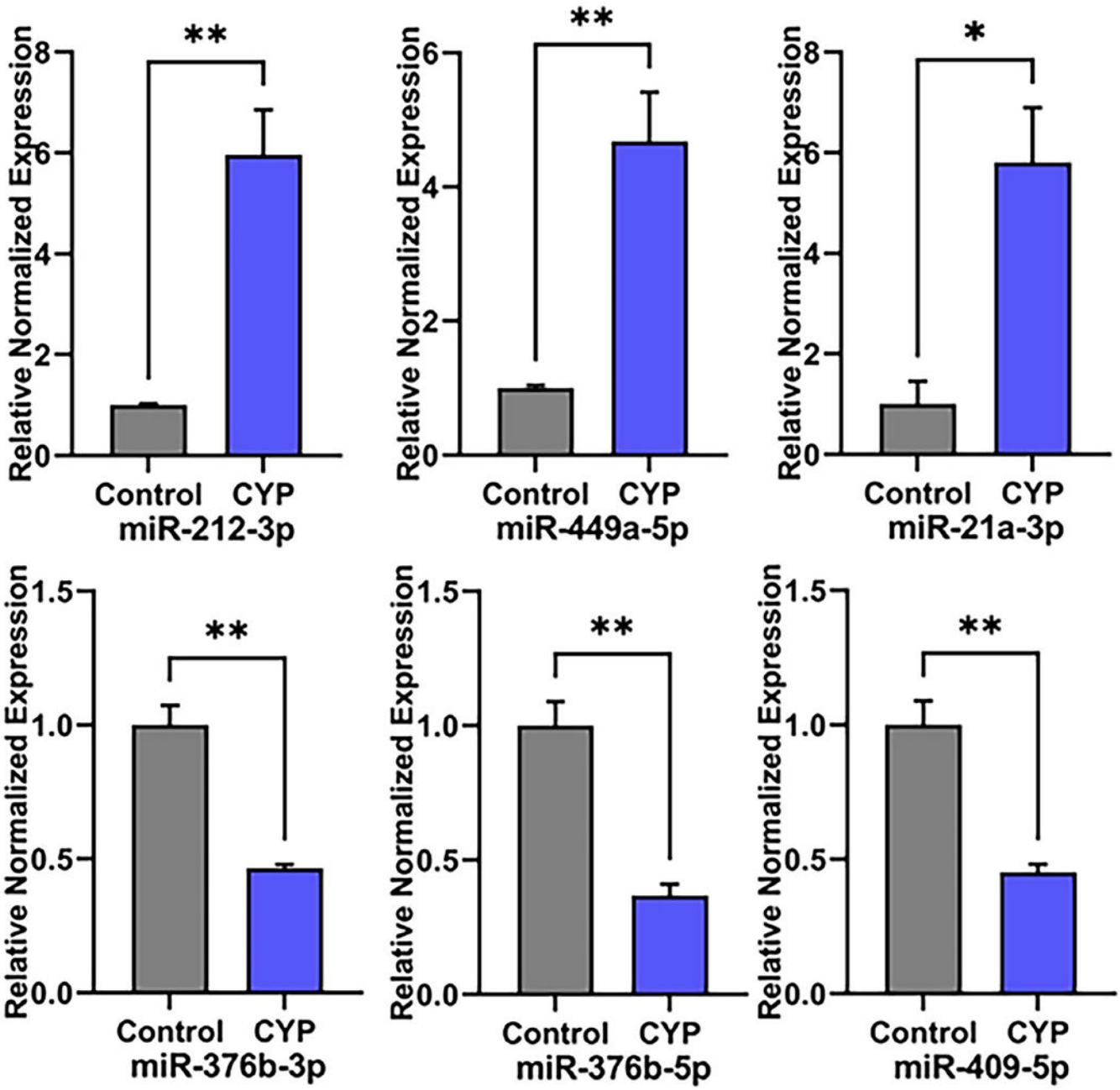

Figure 5. Validation of selected miRs by RT-PCR analysis after CYP-induced cystitis

As shown in the figure is quantitative RT-PCR verifying upregulation of miR-212-3p, miR-449a-5p, and miR-21a-3p and downregulation of miR-376b-3p, miR-376b-5p, and miR-409-5p in UB after CYP induced cystitis. Data are expressed as mean ± SEM. Statistical significance was calculated using the Student's t-test. (⋆p< 0.05 and ⋆⋆ p< 0.01) cystitis vs. control.

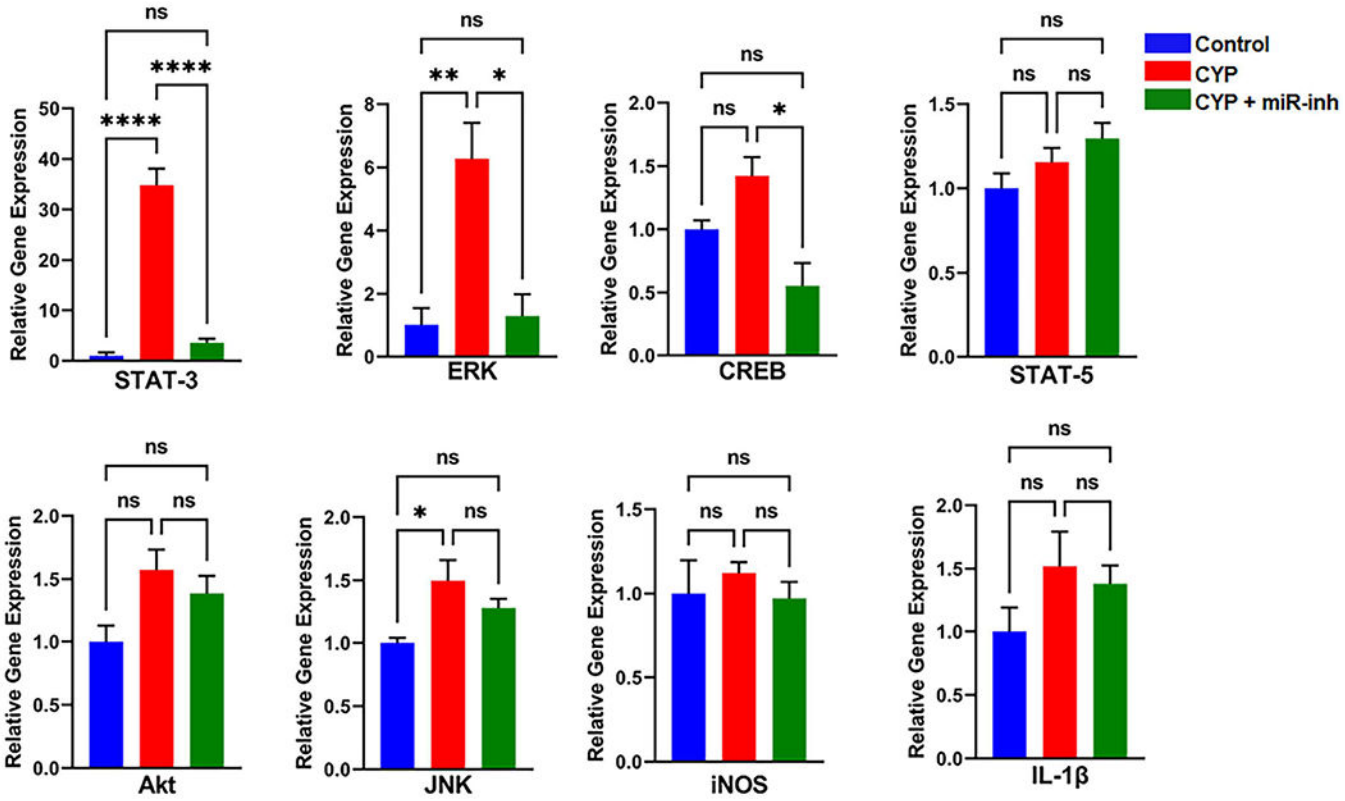

Fig. 6. miR-34c inhibition alters STAT3, ERK, CREB, STAT5, Akt, JNK, iNOS, and IL-1β genes in CYP-induced UB cells

UB cells from CYP-induced cystitis were isolated by regular protocol in our laboratory. These cells were seeded in triplicate in 6 well plates at a density of $0.2x10^6$/well and treated with a combination of miR-34c-inhibitor (10nM final concentration) and Lipofectamine following the manufacturer protocol and incubated for 24 h. Total RNA from each group was isolated, quantitated, reverse-transcribed into cDNA, and analyzed by qPCR with primers specific for STAT3, ERK, CREB, STAT5, Akt, JNK, iNOS, and IL-1β. Data are expressed as mean ± SEM. Statistical significance was calculated using the ANOVA. (ns= not significant $p > 0.05$, *$p< 0.05$, **$p<0.01$ and ****$p<0.0001$).

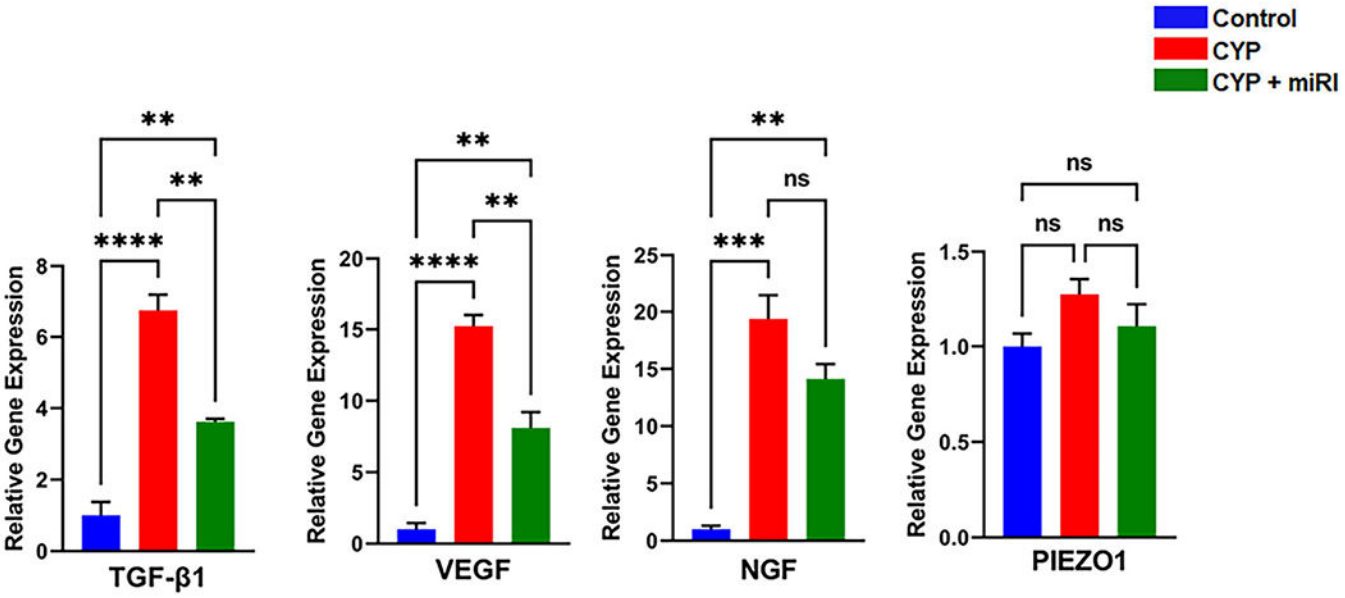

Fig. 7. miR-34c inhibition modulates TGF-β1, VEGF, NGF and PIEZO1 expression

UBs from CYP-induced cystitis were isolated and seeded in triplicate in 6 well plates at a density of $0.2x10^6$/well and, treated with a combination of miR-34c-inhibitor (10nM final concentration) and Lipofectamine following the manufacturer protocol, and incubated for 24 h. Total RNA from each group was isolated, quantitated, reverse-transcribed into cDNA, and analyzed by qPCR with primers specific for TGF-β1, VEGF, NGF, and PIEZO1 expression. Data are expressed as mean ± SEM. Statistical significance was calculated using the ANOVA. (ns= not significant p> 0.05, **p<0.01, ***p<0.001 and ****p<0.0001).

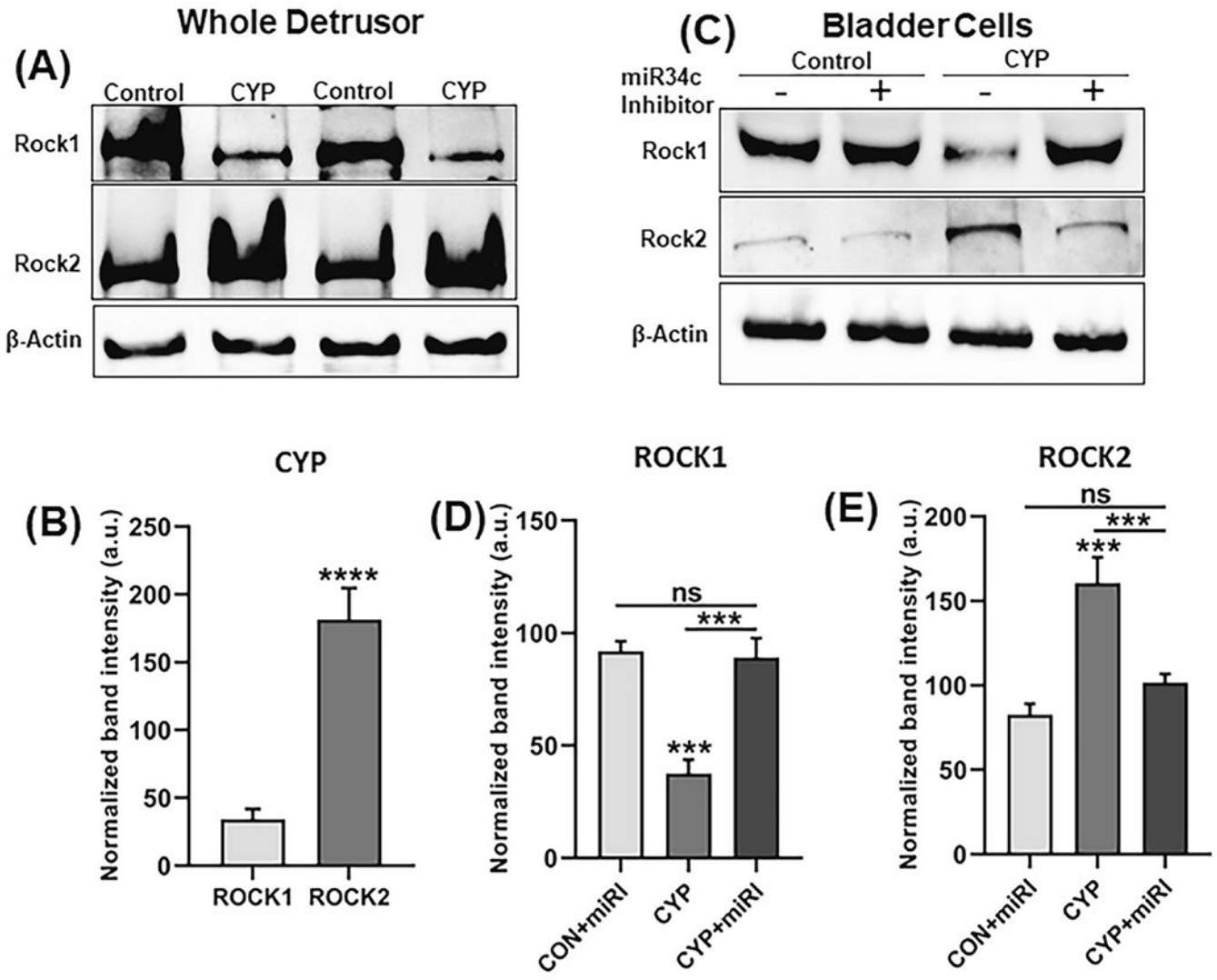

Figure 8. Differential expression of ROCK1 and ROCK2 in detrusor and alteration of these two protein expressions in cystitis bladder cell by miR-34c inhibition

Total protein was isolated from whole detrusor and miR-34c inhibitor-treated CYP-induced cystitis urinary bladder cells (as described in Fig. 6 and 7) by RIPA buffer. Protein concentration was measured and subjected to immunoblot analysis using antibodies specific for ROCK1 and ROCK2. The protein expression was normalized with β-actin expression. (A, B) Immunoblot images and their relative quantification of ROCK1 and ROCK2 in detrusor muscle. ROCK1 decreased and ROCK2 increased in detrusor muscle. (C-E) Immunoblot images and their relative quantification of ROCK1 and ROCK2 in CYP-induced cystitis bladder cells treated with miR-34c antagomir/inhibitor (miRI). ROCK1 and ROCK2 expression reversed after miR-34c inhibitor treatment. Asterisks indicate statistically significant differences between control vs. CYP and CYP vs. miR-34c inhibitor and control vs. miR-34c inhibitor-treated groups. (ns= not significant $p > 0.05$, ***$p<0.001$ and ****$p<0.0001$).

Table 1.

The primer sequence of the gene of interest

Primers	Forward sequence	Reverse Sequence
GAPDH	CATCACTGCCACCCAGAAGACTG	ATGCCAGTGAGCTTCCCGTTCAG
TGF-ß1	TGA TAC GCC TGA GTG GCT GTC T	CAC AAG AGC AGT GAG CGC TGA A
ERK	TGGAAGCCATGAGAGATG	GGTAGAGGAAGTAGCAGATG
CREB	CACAGACCACTGATGGACAGCA	AGGACGCCATAACAACTCCAGG
STAT3	AGG AGT CTA ACA ACG GCA GCC T	GTG GTA CAC CTC AGT CTC GAA G
IL-1β	TGG ACC TTC CAG GAT GAG GAC A	GTT CAT CTC GGA GCC TGT AGT G
STAT5	CTGCTTGCTCAGTCTCTAT	GGCTTCCTCTCCACTATTT
Akt	CTGCTTTGTCATGGAGTATG	CAATCTCCGCACCATAGA
JNK	TTGCCTGTCAGCCTTATC	GCCTACTGCTCATCCTATC
VEGF	CTGCTGTAACGATGAAGCCCTG	GCTGTAGGAAGCTCATCTCTCC
NGF	GTTTTGCCAAGGACGCAGCTTTC	GTTCTGCCTGTACGCCGATCAA
iNOS	GAGACAGGGAAGTCTGAAGCAC	CCAGCAGTAGTTGCTCCTCTTC
PIEZO1	CCTGGAGAAGACTGACGGCTAC	ATGCTCCTTGGATGGTGAGTCC

Table 2.

Primer catalog no of miRs

Name of the miRs	Catalog no. from Qiagen
hsa-miR-34c-5p	YP00205659
mmu-miR-34b-3p	YP00205086
mmu-miR-212-3p	YP00206022
hsa-miR-449a-5p	YP00204481
mmu-miR-21a-3p	YP00205400
mmu-miR-376b-3p	YP00205058
mmu-miR-376b-5p	YP00205199
hsa-miR-409-5p	YP00204014